Free Radical Biology and Medicine 77 (2014) 30–40

Contents lists available at ScienceDirect

Free Radical Biology and Medicine

journal homepage: www.elsevier.com/locate/freeradbiomed

Original Contribution

Kinetic and structural characterization of a typical two-cysteine peroxiredoxin from *Leptospira interrogans* exhibiting redox sensitivity

Diego G. Arias, Anahí Reinoso, Natalia Sasoni, Matías D. Hartman, Alberto A. Iglesias, Sergio A. Guerrero *

Instituto de Agrobiotecnología del Litoral (CONICET), Facultad de Bioquímica y Ciencias Biológicas, Universidad Nacional del Litoral, S3000ZAA Santa Fe, Argentina

ARTICLE INFO

Article history:
Received 28 February 2014
Received in revised form
9 August 2014
Accepted 12 August 2014
Available online 16 September 2014

Keywords:
Leptospira interrogans
Redox-sensitive peroxiredoxin
Thioredoxin system
Peroxide
Free radicals

ABSTRACT

Little is known about the mechanisms by which *Leptospira interrogans*, the causative agent of leptospirosis, copes with oxidative stress at the time it establishes persistent infection within its human host. We report the molecular cloning of a gene encoding a 2-Cys peroxiredoxin (*Lin*AhpC) from this bacterium. After bioinformatic analysis we found that *Lin*AhpC contains the characteristic GGIG and YF motifs present in peroxiredoxins that are sensitive to overoxidation (mainly eukaryotic proteins). These motifs are absent in insensitive prokaryotic enzymes. Recombinant *Lin*AhpC showed activity as a thioredoxin peroxidase with sensitivity to overoxidation by H_2O_2 ($C_{hyp\ 1\%}$ ~30 μM at pH 7.0 and 30 °C). So far, *Anabaena* 2-Cys peroxiredoxin, *Helicobacter pylori* AhpC, and *Lin*AhpC are the only prokaryotic enzymes studied with these characteristics. The properties determined for *Lin*AhpC suggest that the protein could be critical for the antioxidant defense capacity in *L. interrogans*.

Leptospirosis is considered to be the most widespread zoonosis in the world. Human leptospiral infection frequently results in a hard life-threatening illness characterized by liver dysfunction, kidney failure, and pulmonary hemorrhage [1]. The pathogen microorganism *Leptospira interrogans* is particularly adapted to living in the renal tubules of mammals and the treatments for acute cases of leptospirosis have variable effectiveness. Thus, the characterization of specific molecular targets for designing new inhibitors for the bacterium would be useful for developing effective therapies against the disease. Like other infectious agents, survival of *L. interrogans* depends on its ability to evade the oxidative killing mediated by host cells (including macrophages). Curiously, the *L. interrogans* genome has only a few genes putatively involved in resistance to oxidative stress [2]. The bacterium lacks superoxide dismutase, the classical enzyme that detoxifies $O_2^{\cdot-}$; but it possesses catalase, which plays an important role in resistance to oxidative killing by phagocytes [3–5].

The *L. interrogans* genome project reports one gene encoding a typical 2-Cys peroxiredoxin (*Lin*AhpC), which belongs to a widespread family of cysteine-based peroxiredoxins. These proteins exhibit activity against hydrogen peroxide (H_2O_2), organic peroxides, and peroxynitrite, playing an important role in regulating H_2O_2-mediated cell signaling events in eukaryotes [6]. The catalytic cycle of a typical 2-Cys peroxiredoxin consists of three steps: peroxidation, resolution, and recycling. The first step is the oxidation of the peroxidatic Cys (C_P)[1] by the hydroperoxide substrate to a sulfenic acid derivative (C_P-SOH). Next, the C_P-SOH condenses with a second redox-active cysteinyl residue present in another subunit, namely the resolving Cys (C_R), to form an intermolecular disulfide bond. Finally, in the recycling step, this disulfide is reduced by the natural substrate, regenerating free thiol forms of C_P and C_R [6,7]. A second molecule of hydroperoxide can oxidize C_P-SOH to its inactive form of sulfinic acid (C_P-SO_2H), in a reaction that can be reversed only through an ATP-dependent process catalyzed by sulfiredoxin [8]. A large number of studies support the concept that the complex set of reductants (mainly thioredoxin), protein–disulfide oxidoreductase, and associated reductases varies largely with the organism, intracellular location, stage of development, and response to environmental signs [8]. *L. interrogans* lacks genes putatively encoding AhpF, but it presents components of the TRX system [2].

This work focuses on an enzyme that belongs to the AhpC/Prx1 subfamily (herein called *Lin*AhpC), most of which display typical 2-CysPrx mechanisms, with an intermolecular disulfide bond formation [9]. Based on the literature, it is observed that

Abbreviations: TRXR, thioredoxin reductase; TRX, thioredoxin; HEDS, 2-hydroxyethyl disulfide; 2-CysPrx, two-cysteine peroxiredoxin; AhpC, alkylhydroperoxide reductase C; DTT, dithiothreitol; *t*-bOOH, *tert*-butylhydroperoxide; C_P, peroxidatic Cys; C_R, resolving Cys

* Corresponding author. Fax: +54 342 4575221.
E-mail address: sguerrer@fbcb.unl.edu.ar (S.A. Guerrero).

http://dx.doi.org/10.1016/j.freeradbiomed.2014.08.014
0891-5849/

2-CysPrx's (mainly from mammals, plants, and yeasts) exhibiting high sensitivity to overoxidation have two motifs, GGLG and YF, in their primary structure [6,10]. Conversely, in prokaryotes the protein lacks the specified motifs and is much less sensitive to inactivation, except for *Anabaena* and *Helicobacter pylori* 2-CysPrx's, in which recently were found the sequence motifs that make them sensitive to overoxidation by hydroperoxide [11,12]. We show that *L. interrogans* is a new example of a prokaryote having a 2-CysPrx sensitive to overoxidation. Our work contributes to the better understanding of the relevance of the redox metabolism in this pathogen and adds value to the genome project database, identifying the occurrence of functional proteins involved in key metabolic routes.

Materials and methods

Materials

Bacteriological medium components were from Britania Laboratories. Taq DNA polymerase and restriction enzymes were from Fermentas and Promega. All other reagents were of the highest quality commercially available.

Bacteria and plasmids

Escherichia coli Top 10 (Invitrogen) and BL21 (DE3) cells were utilized for plasmid construction and gene expression procedures. The vector pGEM-T Easy (Promega) was selected for cloning and sequencing purposes, whereas the expression vector was pET28c (Novagen). Genomic DNA from *L. interrogans* was obtained using a Wizard genomic DNA purification kit (Promega). DNA manipulation, *E. coli* culture, and transformation were performed according to standard protocols.

Culture of L. interrogans

Bacteria were grown in Ellinghausen–McCullough–Johnson–Harris medium supplemented with bovine serum albumin and Tween 80 at pH 7.4 [13,14]. Static cultures were incubated for 3–5 days at 28 °C. The cell density was recorded at 420 nm in an S-26 spectrophotometer (Boeco Germany). The number of bacteria was estimated according to Louvel and Picardeau [15], by which $0.3\ OD_{420\ nm} \cong 6.0 \times 10^8$ bacteria ml^{-1}.

Molecular cloning of lin2-cysprx and construction of the expression vector

The *2-cysprx* gene from *L. interrogans* was amplified from its respective genomic DNA by PCR, using the following oligonucleotide primer pair designed from the known sequence (*L. interrogans* serovar Copenhageni Genome Project, http://aeg.lbi.ic.unicamp.br/world/lic/): forward, *GCTAGCGGATCC*ATGCCTCAGGTCACATCTTTAG; reverse, *AAGCTT*TCAATTCACGGCAGCAAAGT.

PCR was performed under the following conditions: 94 °C for 10 min; 30 cycles of 94 °C for 1 min, 50 °C for 1 min, and 72 °C for 1 min; and then 72 °C for 10 min. The PCR product was subsequently purified and ligated into the pGEM-T Easy vector (Promega) to facilitate further work. The fidelity and correctness of the cloned gene were confirmed on both strands by complete sequencing (Macrogen). The construction obtained was digested with the enzymes *Nhe*I and *Hin*dIII and purified by gel extraction after gel electrophoresis. The purified insert was ligated to the pET28c vector (Novagen) using T4 DNA ligase for 16 h at 16 °C. Competent *E. coli* BL21 (DE3) cells were transformed with the construct. Transformed cells were selected in agar plates containing Luria–Bertani broth (LB; 10 g L^{-1} NaCl, 5 g L^{-1} yeast extract, 10 g L^{-1} peptone, pH 7.4) supplemented with kanamycin (50 μg ml^{-1}). Preparation of plasmid DNA and subsequent *Nhe*I/*Hin*dIII restriction enzyme treatment were performed to check the correctness of the construct.

Overexpression and purification of recombinant LinAhpC

A single colony of *E. coli* BL21 (DE3) transformed with pET28c/*Lin*AhpC was selected and an overnight culture was diluted 1/100 in fresh medium (LB broth supplemented with 50 μg ml^{-1} kanamycin) and grown under identical conditions to exponential phase, $OD_{600} \sim 0.6$. The expression of the respective recombinant protein was induced with 0.5 mM isopropyl-β-D-1-thiogalactopyranoside (IPTG), followed by incubation at 28 °C. After 16 h the cells were harvested and stored at −20 °C. Purification of *Lin*AhpC was performed using a Ni^{2+}–IDA–agarose resin (Hi Trap chelating HP; GE Healthcare). Briefly, the bacterial pellet was resuspended in binding buffer (20 mM Tris–HCl, pH 7.5, 400 mM NaCl, and 10 mM imidazole) and disrupted by sonication. The lysate was centrifuged (10,000*g*, 30 min) to remove cell debris. The resultant crude extract was loaded onto the Ni^{2+}–IDA–agarose column, which had been equilibrated with binding buffer. After being washed with 10 bead volumes of the same buffer, the recombinant protein was eluted with elution buffer (20 mM Tris–HCl, pH 7.5, 400 mM NaCl, 300 mM imidazole). Fractions containing pure protein were pooled, concentrated, and frozen with glycerol at −80 °C. TRX from *E. coli* (*Eco*TRX) was purified from *E. coli* BL21 (DE3) cells transformed with the commercial pET32a plasmid (Novagen) under the same conditions as *Lin*AhpC. TRX reductase from *E. coli* (*Eco*TRXR) was expressed in *E. coli* DH5α [pTR301/*Ec*TRXR] and purified according to the protocol described by Holmgren and Bjornstedt [16].

Protein methods

Proteins were analyzed by native PAGE and SDS–PAGE using the Mini-Protean II (Bio-Rad) apparatus [17]. The final polyacrylamide monomer concentration was 15% (w/v) for the separating gel and 4% (w/v) for the stacking gel. Coomassie brilliant blue was used for protein staining. Native PAGE (in the absence of SDS) was performed using the Mini-Protean II (Bio-Rad) apparatus. The final polyacrylamide monomer concentration was 8% (w/v) at pH 8.8 [18]. Coomassie brilliant blue was used for protein staining. Protein concentration was determined by the method of Bradford with bovine serum albumin as standard [19]. Protein thiols were quantified with 5,5-dithiobis-2-nitrobenzoic acid (DTNB; $\varepsilon_{412\ nm} = 14.15\ mM^{-1}\ cm^{-1}$) in 100 mM Tris–HCl, pH 7.5 [20].

Serum anti-*Lin*AhpC was prepared by immunization of a rabbit with the purified recombinant proteins according to Vaitukaitis et al. [21]. Bacterial protein extracts were prepared by resuspending the parasite pellets in lysis buffer (50 mM Tris–HCl, pH 7.5, 1% SDS). Proteins in an SDS–PAGE gel were blotted onto a nitrocellulose membrane. The membrane was blocked overnight at 4 °C, subsequently incubated with primary antibody at room temperature for 1 h, and then incubated with a horseradish peroxidase (HRP)-conjugated anti-rabbit secondary antibody for 1 h. Bands were visualized using an ECL Western blotting detection reagent (Thermo Scientific). Estimation of the relative abundance of *Lin*AhpC in *L. interrogant* protein extracts was performed using Western blots of total cell lysates from the bacteria cultivated under standard conditions. The *Lin*AhpC cellular content was derived from the standard line constructed with the integrated optical densities of each band versus the amounts of recombinant *Lin*AhpC. In our hands, comparison analysis between bands obtained in the absence or presence of DTT estimated approximately the same amount of protein (that is, the quantification of

the dimer in the absence of DTT gave about the same amount as that of the dimer + monomer in its presence).

Enzyme assays

Peroxidase activity was measured by monitoring NADPH oxidation at 340 nm by means of a coupled assay that guaranteed the regeneration of *Eco*TRX in its reduced form. All enzyme assays were performed at 30 °C, in a final volume of 50 μl and using a Multiskan Ascent one-channel vertical light-path filter photometer (Thermo Electron Co.). The reaction mixture contained (unless otherwise specified) 100 mM potassium phosphate, pH 7.0, 2 mM EDTA, 200 μM NADPH, 1 μM *Eco*TRXR, 10 μM *Eco*TRX, and *Lin*AhpC (in a specific concentration range, 0.05–5 μM). Reactions were started by the addition of 100 μM H_2O_2 or *tert*-butylhydroperoxide (*t*-bOOH). For steady-state kinetic analysis, assays were performed using 0.3–20 μM *Eco*TRX and 1.5–25 μM H_2O_2 or *t*-bOOH. Glutathione-dependent assays were performed as for the TRX-dependent assays in a volume of 50 μl, at 30 °C, in medium containing 100 mM potassium phosphate, pH 7.0, 2 mM EDTA, 0.2 mM NADPH, 2 U ml^{-1} glutathione reductase (from *Saccharomyces cerevisiae;* Sigma), 3 mM glutathione (GSH), 0.05–5 μM *Lin*AhpC, and 100 μM H_2O_2. Kinetic data were plotted as initial $v \times [LinAhpC]^{-1}$ (min^{-1}) versus substrate concentration (μM). The kinetic constants were acquired by fitting the data with a nonlinear least-squares formula and the Michaelis–Menten equation using the program Origin 7.0. Kinetic constants were the means of at least three independent sets of data, and they were reproducible within ± 10%.

Gel filtration chromatography

The M_r of *Lin*AhpC (~40 μM) was assayed by gel filtration chromatography in a Superdex 200 HR Tricorn column (GE) equilibrated at a flow rate of 0.5 ml min^{-1} with 50 mM Hepes buffer, pH 8.0, containing 100 mM NaCl and 0.1 mM EDTA. The calibration curve was constructed using the logarithm of the M_r (log M_r) vs the distribution coefficients (K_{av}) measured for each M_r standard: thyroglobulin (669 kDa), ferritin (440 kDa), aldolase (158 kDa), conalbumin (75 kDa), ovalbumin (43 kDa), carbonic anhydrase (29 kDa), ribonuclease A (13.7 kDa), and aprotinin (6.5 kDa) (gel filtration calibration kit; GE). The distribution coefficient was defined as $K_{av} = (V_e - V_o)/(V_T - V_o)$, where V_e is the elution volume, V_T is the total column volume, and V_o is the exclusion volume.

Determination of the redox potential

Redox titration was carried out by incubating the protein (5 μM) for 4 h at 30 °C in a reaction mixture containing 100 mM Tris–HCl, pH 7.5, and variable molar ratios of β-mercaptoethanol/HEDS (total concentration of 100 mM) to reach different half-cell potentials (E_h) according to the Nernst equation [22]. After incubation, protein thiols were blocked with 10 mM iodoacetamide and the samples were analyzed by nonreducing SDS–PAGE. The respective reduced (monomeric) fraction was estimated by densitometry, using the program Lab-Image 2.7.2 (Kapelan GmbH). The titration curve was fitted as a reduced fraction vs E_h. The standard reduction potential ($E_{m7.5}$) was determined by nonlinear regression treatment of the data according to a logistic model using the program Origin 7.0.

Measurement of the thiolate anion by UV absorption

Previous to the analysis, *Lin*AhpC was reduced with 50 mM DTT for 15 min, and then the excess of DTT was removed using a Sephadex G-25 column preequilibrated with 50 mM Tris–HCl, pH 7.5, 1 mM EDTA, 100 mM NaCl. The pH-dependent Cys ionization was followed by the absorption of the thiolate anion at 240 nm. Spectra of either oxidized or reduced protein (~5–10 μM) were recorded between 200 and 340 nm at various pH values (from 4.5 to 10). Proteins were diluted (1/200) at 25 °C in 1 ml of medium containing 100 mM potassium phosphate buffer at the respective pH. The final protein concentration (reduced and oxidized forms) was normalized using the absorbance A_{280}. Values of pH were checked after the addition of the protein. Spectra were measured against buffer solution in a stoppered quartz cuvette in a Boeco S-26 UV–Vis spectrophotometer and A_{240} was converted into the molar extinction coefficient (ε_{240}). The $\Delta\varepsilon_{240}$ values (ε_{240} (reduced form) − ε_{240} (oxidized form)) were plotted against pH and the pK_a value was determined by direct fit to the Henderson–Hasselbalch equation [23–25].

Stress resistance assays

For a disk inhibition assay, recombinant *E. coli* cells (transformed with empty pET28c vector or the pET28c/*Lin*AhpC construct) were grown overnight at 37 °C in LB broth containing kanamycin (50 μg ml^{-1}) and then normalized to an OD_{630} of 0.1. An aliquot of these cells (200 μl) was diluted in fresh top agar (LB-agar 0.65% w/v in the presence of 0.1 mM IPTG and 50 μg ml^{-1} kanamycin) and placed in a petri dish. A sterilized filter disk (6 mm in diameter) was placed in the middle of the plate and soaked with 5 μl of either 1 mM H_2O_2 or 0.5 mM *t*-bOOH. Plates were incubated overnight at 37 °C [26].

To test growth rate under stress conditions, recombinant *E. coli* cells were grown in fresh LB medium containing kanamycin (50 μg ml^{-1}) at 37 °C until the log phase was reached. Then, the cultures were normalized to OD_{630} ~0.05 and grown in the presence of 0.1 mM IPTG for 30 min at 37 °C. Then, the cultures were further grown in the absence or presence of 1 mM H_2O_2 and followed by measurement of OD_{630} at various time intervals.

LinAhpC overoxidation detection in vivo

Exponential *L. interrogans* cells harvested by centrifugation at 10,000*g* for 10 min at 25 °C were washed twice with phosphate-buffered saline (PBS; 8 g L^{-1} NaCl, 0.2 g L^{-1} KCl, 1.44 g L^{-1} Na_2HPO_4, 0.24 g L^{-1} KH_2PO_4, pH 7.4)) to remove residual medium components. The cells were incubated in PBS buffer (at final $OD_{420\ nm}$=1) with various concentrations of H_2O_2 (0, 5, 10, and 50 mM) for 1 and 3 h at 28 °C. Subsequently, the cells were harvested and disrupted with nonreducing SDS–PAGE buffer. Protein extracts were analyzed by Western blot using anti-*Lin*AhpC or anti-lipoprotein 32 (LP32) as primary antibodies and HRP-conjugated anti-rabbit as secondary antibody. Bands were visualized using the ECL Western blotting detection reagents (Thermo Scientific).

Phylogenetic analysis of 2-CysPrx from eukaryotic and prokaryotic organisms

Amino acid sequences were obtained from the National Center for Biotechnology Information (NCBI) protein database (http://www.ncbi.nlm.nih.gov/). Sequences were aligned with Muscle (http://www.ebi.ac.uk/Tools/msa/muscle/) and alignment was analyzed and edited with BioEdit 7.0.5.3 (Hall 1999). Afterward, the alignment was cured using Gblocks (http://www.phylogeny.fr/version2_cgi/one_task.cgi?task_type=gblocks), and the ProtTest server (http://darwin.uvigo.es/software/prottest_server.html) was used to select the model of protein evolution that best fit the cured alignment. Tree reconstruction was performed with Seaview 4.4

[27] using the LG method and a bootstrap of 1000. The tree was prepared in the FigTree 1.4 program (http://tree.bio.ed.ac.uk/).

Results

Bioinformatics analysis of LinAhpC

In the database of the *L. interrogans* serovar Copenhageni genome project (http://aeg.lbi.ic.unicamp.br/world/lic/) a sequence encoding a putative typical 2-Cys peroxiredoxin (*Lin*AhpC, LIC11219), belonging to the AhpC/Prx1 subfamily [9], was identified. In addition, other sequences encoding other peroxiredoxin proteins are present in the genome of this bacterium: btuE (glutathione peroxidase-like protein, LIC12648), Gpo (glutathione peroxidase-like protein, LIC13442), TPx (thiol peroxidase, LIC12765), and two bacterioferritin comigratory proteins (LIC20093 and LIC10732). Based on bioinformatics analysis, an alignment of the *Lin*AhpC amino acid sequence showed a high sequence identity with other 2-CysPrx's, including the two redox-active sites containing key cysteine residues (Fig. 1). It also contains a conserved catalytic C_P (Cys^{48}) and a C_R (Cys^{168}) at the N- and C-terminal region, respectively. Results in Fig. 1 indicate that *Lin*AhpC is a member of the AhpC-like protein subfamily (within the typical 2-CysPrx category), and it is also related to the group of 2-CysPrx's sensitive to overoxidation. *Lin*AhpC showed conservation of the motifs GG(L/V/I)G (especially GGVG) and YF (mainly found in eukaryotes) correlated with sensitivity to inactivation [6,7], as depicted in Fig. 2. In addition, the phylogenetic analysis revealed an association between *Lin*AhpC and the enzyme group sensitive to overoxidation. The *L. interrogans* protein exhibited a high degree of identity with 2-CysPrx's from eukaryotic organisms such as *Homo sapiens* Prx2 (60.6%), Prx1 (54.8%), and Prx4 (39.1%); *Mus musculus* Prx2 (60.1%); *Pisum sativum* 2-CysPrx (42%); and *Sac. cerevisiae* TSA1 (55.1%).

Expression and characterization of recombinant LinAhpC

The identification of a nucleotide sequence encoding a putative *Lin*AhpC in the database of the *L. interrogans* genome project prompted us to perform the molecular cloning of the respective gene. After amplification of the gene from the genomic DNA, its identity was confirmed by DNA sequencing. To further seek the functionality of *Lin*AhpC the amplified gene was cloned into the vector pET28c and expressed in *E. coli* BL21 (DE3) to produce the respective recombinant protein fused to an N-terminal 6× His-tag. The soluble fraction was purified chromatographically onto a Ni^{2+}-affinity resin, to reach purity higher than 95%, as judged by SDS–PAGE analysis shown in Supplementary Fig. 1. The M_r thus revealed (24 kDa) for the *Lin*AhpC fully agrees with the expected size deduced from their DNA-derived amino acid sequence plus ~2 kDa of residues contained in the His-tag.

LinAhpC displays TRX peroxidase activity

As a first approach to analyzing the functionality of the recombinant *Lin*AhpC, assays of disk inhibition and growth under oxidative stress were performed to test whether expression of the protein modified the capacity of *E. coli* cells to cope with oxidant conditions (Fig. 3). Inhibition rings were observed in the presence of either 1 mM H_2O_2 or 0.5 mM *t*-bOOH but, as shown in Fig. 3A, plates containing *E. coli* cells transformed to produce *Lin*AhpC

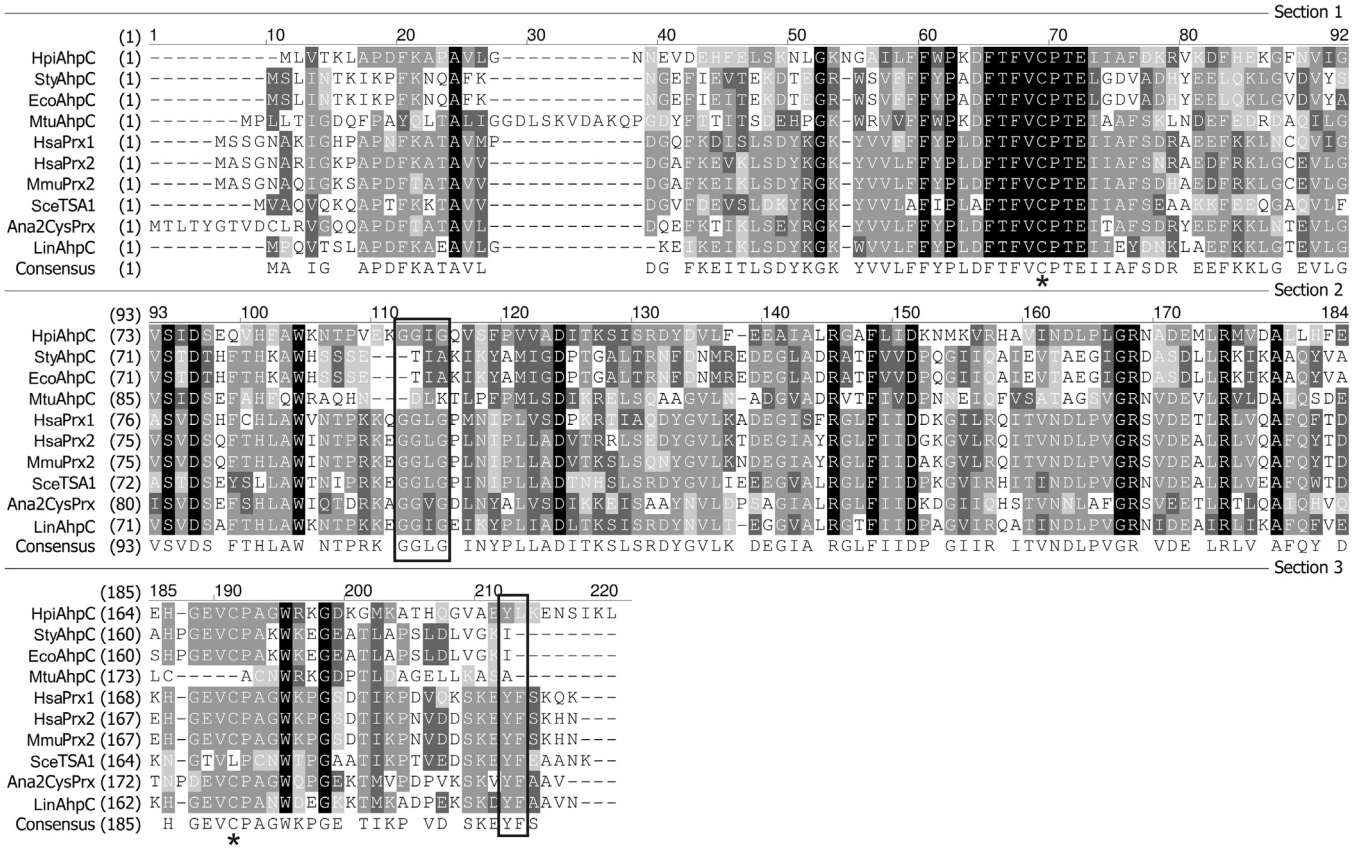

Fig. 1. Amino acid sequence alignment of *Lin*AhpC with typical 2-CysPrx orthologs belonging to the AhpC/Prx1 group: *Helicobacter pylori* AhpC, *Salmonella typhimurium* AhpC, *Escherichia coli* AhpC, *Mycobacterium tuberculosis* AhpC, *Homo sapiens* Prx1, *H. sapiens* Prx2, *Mus musculus* Prx2, *Saccharomyces cerevisiae* TSA1, and *Anabaena* 2-CysPrx. Each individual sequence is numbered accordingly. The black box indicates the amino acid motif responsible for overoxidation sensitivity and the asterisks indicate the redox-active cysteine residues. For details, see Supplementary Table 1.

had rings with a smaller diameter than control plates (*E. coli* cells transformed with pET28c alone), thus indicating enhanced tolerance to oxidative damage. Also, the growth rate of *E. coli* cells overexpressing 2-CysPrx was higher than in the control culture (Fig. 3B). These results confirm the *Lin*AhpC peroxidase activity in vivo and suggest the capacity of the *Eco*TRX system to reduce *Lin*AhpC.

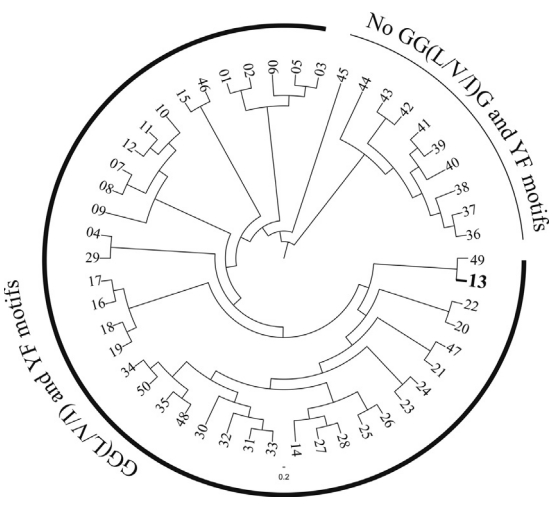

Fig. 2. Phylogenetic analysis of *Lin*AhpC. Amino acid sequences of AhpC/Prx1 group members were obtained from the NCBI protein database (see supplementary material). Multiple sequence alignments were done with the Muscle program. Tree reconstruction was performed with Seaview 4.4 using the LG method and a bootstrap of 1000. The tree was prepared in the FigTree 1.4 program. For details, see Supplementary Table 1. 1, *Riccia fluitans;* 2, *Anabaena vairabilis;* 3, *Pisum sativum;* 4, *Trypanosoma cruzi;* 5, *Arabidopsis thaliana;* 6, *A. thaliana;* 7, *Plasmodium falciparum;* 8, *Plasmodium berghei;* 9, *Cryptosporidium parvum;* 10, *Helicobacter pylori;* 11, *Pseudomonas putida;* 12, *Vibrio cholera;* 13, *Leptospira interrogans;* 14, *Giardia lamblia;* 15, *Entamoeba histolytica;* 16, *Schistosoma mansoni;* 17, *Homo sapiens;* 18, *H. sapiens;* 19, *Mus musculus;* 20, *M. musculus;* 21, *M. musculus;* 22, *Bos taurus;* 23, *Caenorhabditis elegans;* 24, *Haemonchus contortus;* 25, *Saccharomyces cerevisiae;* 26, *Schizosaccharomyces pombe;* 27, *Taenia crassiceps;* 28, *Echinococcus granulosus;* 29, *Leishmania donovani;* 30, *Schistosoma japonicum;* 31, *Schistosoma mansoni;* 32, *Fasciola hepatica;* 33,, *Opisthorchis viverrini;* 34, *Trypanosoma brucei;* 35, *Crithidia fasciculata;* 36, *Escherichia coli;* 37, *Salmonella typhimurium;* 38, *Xylella fastidiosa;* 39, *Amphibacillus xylanus;* 40, *Streptococcus pyogenes;* 41, *Staphylococcus aureus;* 42, *Clostridium perfringens;* 43, *Treponema pallidum;* 44, *Desulfovibrio vulgaris;* 45, *Mycobacterium tuberculosis;* 46, *Babesia bovis;* 47, *Thunnus maccoyii;* 48, *Leishmania infantum;* 49, *Phanerochaete chrysosporium;* 50, *T. cruzi.*

Based on the above results, the peroxidase activity of His-tagged *Lin*AhpC was analyzed in vitro using a heterologous NADPH-dependent TRX system (TRXR and TRX) from *E. coli*. In this coupled assay, the rate of H_2O_2 or *t*-bOOH reduction was dependent on the His-tagged *Lin*AhpC concentration, *Eco*TRX being an essential reducing substrate for this enzymatic system (Supplementary Fig. 2). No peroxidase activity was detected when the TRX system was replaced with GSH and glutathione reductase (data not shown). These results suggest that *Lin*AhpC uses TRX (or another putative thiol-dependent redoxin) as a necessary mediator for the electron transfer, especially taking into account that *L. interrogans* lacks AhpF genes.

Steady-state kinetic assays revealed that the reaction of peroxide reduction catalyzed by His-tagged *Lin*AhpC with *Eco*TRX follows an apparent hyperbolic mechanism (Supplementary Fig 2). The catalytic efficiency ($k_{cat}\ K_m^{-1}$) calculated for peroxide reduction is similar for both peroxides, which might indicate a sort of promiscuity for the use of substrate, this being common for this type of enzyme. Table 1 shows the apparent kinetic parameters for TRX-dependent reduction of H_2O_2 and *t*-bOOH by His-tagged *Lin*AhpC. Alternatively, the kinetic parameters for the substrate TRX (*Eco*TRX) were evaluated using both H_2O_2 and *t*-bOOH, and the enzymatic efficiencies ($k_{cat}\ K_m^{-1}$) for TRX oxidation were not modified appreciably (Table 1).

Table 1
Apparent kinetic parameters of recombinant His-tagged *Lin*AhpC, determined at 30 °C and pH 7.0.

Cosubstrate	Substrate	$k_{cat\ app}$ (min^{-1})	$K_{m\ app}$ (μM)	$k_{cat}\ K_m^{-1}$ ($M^{-1}\ s^{-1}$)
*Eco*TRX 10 μM	H_2O_2	102 ± 12	5 ± 2	3.4×10^5
*Eco*TRX 10 μM	*t*-bOOH	150 ± 5	3.3 ± 0.9	7.6×10^5
H_2O_2 100 μM	*Eco*TRX	122 ± 5	3.1 ± 0.5	6.5×10^5
t-bOOH 100 μM	*Eco*TRX	200 ± 14	5 ± 1	6.7×10^5

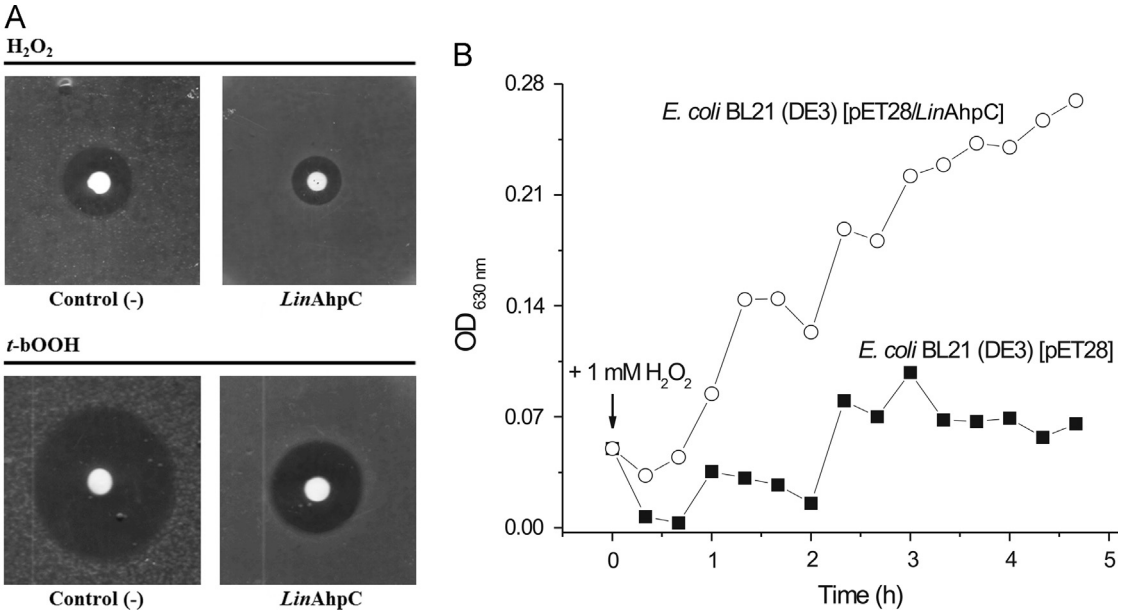

Fig. 3. Effect of peroxides on growth of transformed *E. coli*. (A) Disk inhibition assay. The top row shows transformed *E. coli* supplemented with 5 μl of 1 mM H_2O_2. The bottom row shows the growth of bacteria treated with 5 μl of 0.5 mM *t*-bOOH. Left columns represent pET28c vector-transformed *E. coli*. Right columns indicate the pET28c/*Lin*AhpC-transformed strain. (B) The growth profile of the *E. coli* cells after the addition of 1 mM H_2O_2 (arrow).

LinAhpC is sensitive to overoxidation by peroxide substrate in vitro

The effects of variable levels of peroxide on the peroxidase activity of His-tagged *Lin*AhpC were evaluated using an enzymatic coupled assay in the 25–400 μM range of H_2O_2 concentration (Fig. 4). As shown in Fig. 4A, at low H_2O_2 concentrations (up to 50 μM) consumption of NADPH kept a stoichiometric relationship with the peroxide. However, at high H_2O_2 concentrations (100 μM or higher), a notable reduction in the reaction rate and a loss of stoichiometry with NADPH consumed were observed. These results suggest a possible inhibition/inactivation of His-tagged *Lin*AhpC that is dependent on time and peroxide concentration. Interestingly, no difference in overoxidation sensitivity profile was observed when the His-tag was removed in the recombinant protein (Supplementary Fig. 3). This result indicates that an N-terminal His-tag has no effect on the sensitivity properties of this 2-CysPrx.

As has been previously described in the literature [28], the fraction of peroxiredoxin that is inactivated during each catalytic cycle can be described by

$$f_{\text{inact}} = \frac{k_{SO_2H} \cdot [H_2O_2]}{k_{SO_2H} \cdot [H_2O_2] + k_{SS} \cdot K_{LU}}$$

where k_{SO2H} is the rate constant for sulfinic acid formation, k_{SS} is the rate constant for disulfide bond formation, and K_{LU} is the equilibrium constant for locally unfolded relative to fully folded enzyme. When f_{inact} is < 0.1, the above relationship can be approximated as

$$f_{\text{inact}} \approx \frac{k_{SO_2H} \cdot [H_2O_2]}{k_{SS} \cdot K_{LU}}$$

the slope of the f_{inact} vs $[H_2O_2]$ line being the peroxide sensitivity, which approximates $k_{SO2H}\ k_{SS}^{-1}\ K_{LU}^{-1}$. The inverse of this slope divided by 100 corresponds to the peroxide concentration (in μM) at which 1 of every 100 *Lin*AhpC (1%) is inactivated (by overoxidation) per turnover. As shown in Fig. 4B, f_{inact} showed a linear relationship with the H_2O_2 concentration. The H_2O_2 concentration that inactivated the 1% of *Lin*AhpC ($C_{\text{hyp 1\%}}$) was calculated to be ~30 μM (at pH 7.0 and 30 °C). This calculated value is slightly lower than the estimated $C_{\text{hyp 1\%}}$ for human Prx1 with H_2O_2 ($C_{\text{hyp 1\%}} = 62$ μM [28]). This would indicate that *Lin*AhpC is sensitive to peroxide-dependent inactivation.

To support the hypothesis of a possible peroxide substrate-dependent inactivation (as detailed by Nelson et al. [28]), the TRX peroxidase activity of His-tagged *Lin*AhpC, its thiol group content, and the covalent dimeric state of the protein were evaluated after incubating the protein with H_2O_2 and/or DTT (Fig. 5). As a control, the protein was incubated under identical conditions in the absence of redox reagents. A slight reduction in peroxidase activity, as well as covalent dimeric migration (in nonreducing SDS–PAGE), was observed when the protein was incubated only with H_2O_2 (Fig. 5A and B), indicating the presence of intermolecular disulfide bonds. The protein treated with the combination of DTT and peroxide exhibited a major loss of activity (Fig. 5A), as well as monomeric migration (and no thiol detection) in nonreducing SDS–PAGE (Fig. 5B). Accordingly, thiol groups per monomer determined for the reduced, oxidized, or overoxidized protein were 2.1 ± 0.1, 0.1 ± 0.1, and 0.9 ± 0.2, respectively. These results suggest that the loss of activity is associated with the change in the redox state of cysteine residue (overoxidation) and the protein oligomeric structure. A similar profile was observed for the titration of His-tagged *Lin*AhpC monomer/dimer at various H_2O_2 concentrations in the presence of 10 or 100 mM DTT (Fig. 6A). At high concentrations of H_2O_2 and DTT, the monomeric (inactive) form of His-tagged *Lin*AhpC was generated (Fig. 6B). Similar results were obtained when H_2O_2 was replaced with *t*-bOOH (data not shown). Our results suggest that the peroxide-dependent inactivation of His-tagged *Lin*AhpC is caused by overoxidation of its C_P (as C_P-SOH) to C_P-SO_2H or C_P-SO_3H. As previously described for other sensitive 2-CysPrx's, this redox modification prevents the formation of a covalent dimer by disulfide bond during the catalytic cycle and is responsible for inactivation of the peroxidase activity [28,29].

Additional evaluation of the redox-dependent oligomeric state of His-tagged *Lin*AhpC by gel filtration chromatography showed that it arranges in a stable decameric (or pentadimeric) form (apparent M_r ~240 kDa) when fully reduced with DTT (Fig. 7A and B). After oxidation of the enzyme with H_2O_2, a mixture of oligomeric protein species was observed, with the majority in a dimeric form (apparent M_r ~51 kDa) and a lesser proportion in the decameric form of the protein. After the overoxidation of *Lin*AhpC, an oligomeric species was observed, which did not fit well to single- or two-species models (apparent M_r ~37 kDa, Fig. 7A and B), suggesting the possible presence of a range of species. A similar profile was observed in His-tagged *Lin*AhpC

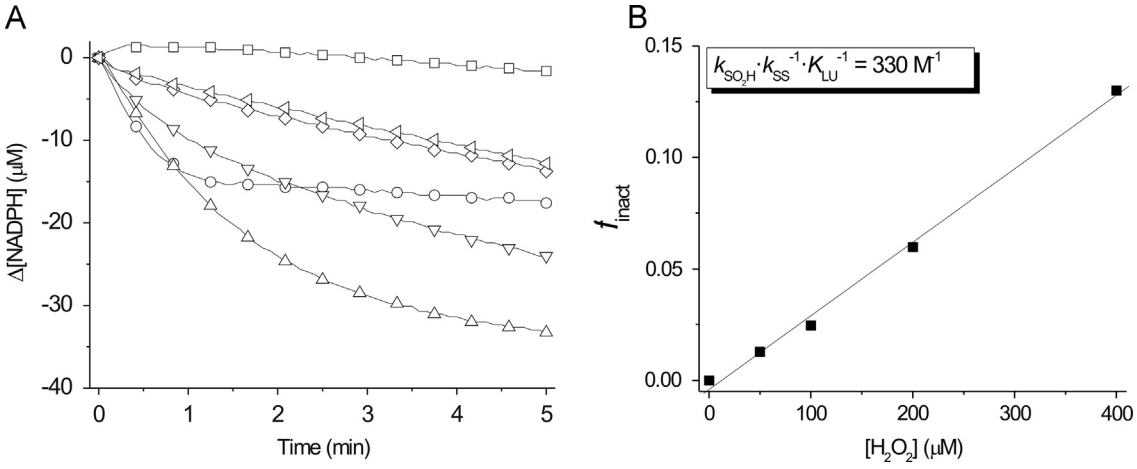

Fig. 4. Inactivation kinetics of His-tagged *Lin*AhpC by H_2O_2. (A) Time course for NADPH oxidation at various H_2O_2 concentrations, (□) 0 μM, (○) 12 μM, (Δ) 25 μM, (▽) 50 μM, (◇) 100 μM, and (◁) 200 μM, in presence of 10 μM *Eco*TRX and 0.1 μM His-tagged *Lin*AhpC. Data were plotted and used for curve fitting using an equation described in the text. (B) Replot of f_{inact} (inactivated fraction of *Lin*AhpC under turnover) as a function of H_2O_2 concentration. The linear fit provides an estimate of the $k_{SO2H}\ k_{SS}^{-1}\ K_{LU}^{-1}$ relation. Details for the analyses are described in the text.

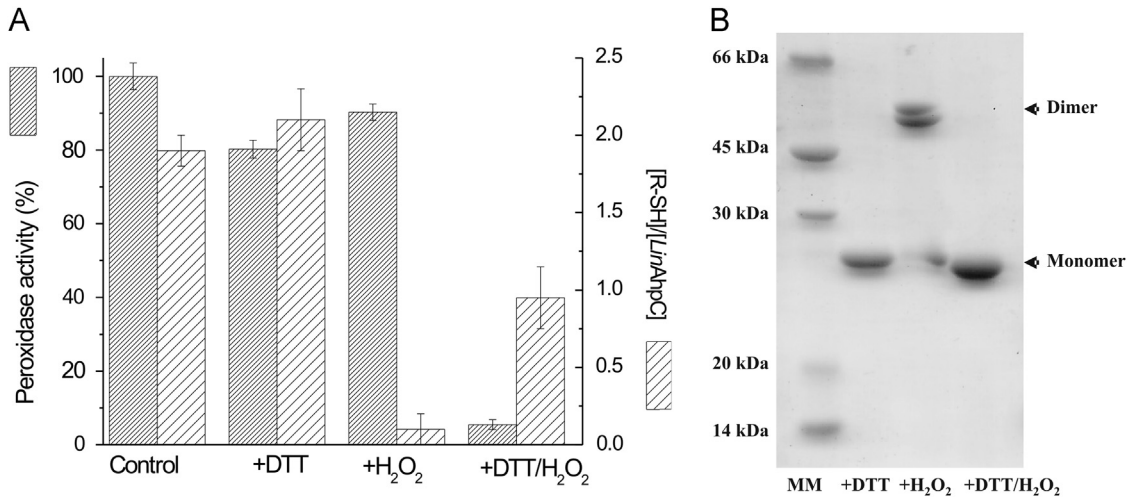

Fig. 5. Redox-dependent inactivation of His-tagged *Lin*AhpC. (A) Residual TRX peroxidase activity of His-tagged *Lin*AhpC and thiol titration (with DTNB reagent) after incubation under various redox conditions. The protein was incubated with 10 mM DTT, 0.5 mM H_2O_2, or 10 mM DTT plus 20 mM H_2O_2 for 10 min at 25 °C and pH 7.5. After desalting (using gel filtration chromatography with Sephadex G-25) the activity was determined as described under Materials and methods. As an experimental control, *Lin*AhpC was incubated in the absence of redox reagents. (B) Nonreducing SDS–PAGE of treated His-tagged *Lin*AhpC.

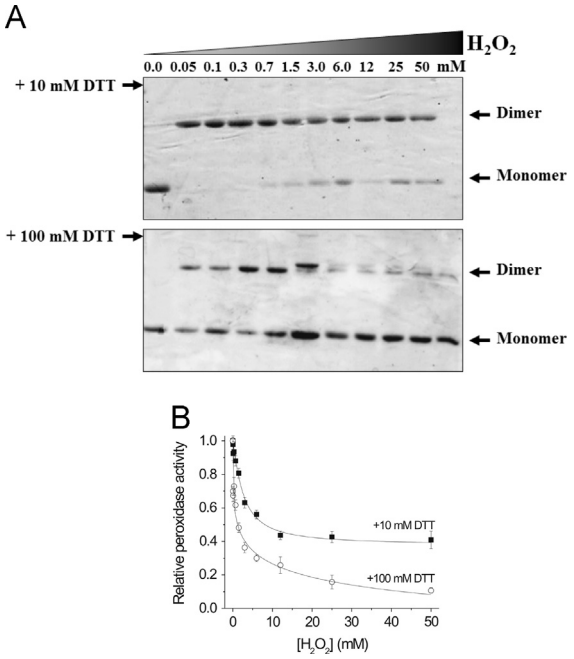

Fig. 6. Overoxidation sensitivity of His-tagged *Lin*AhpC. Protein (10 μM) in standard assay buffer was reduced with 10 or 100 mM DTT for 5 min at 25 °C. Subsequently, aliquots were mixed with various concentrations of H_2O_2 (from 0.05 to 50 mM) at 25 °C. After 15 min, samples of each reaction mixture were: (A) denatured by adding nonreducing sample loading buffer (in the presence of 20 mM iodoacetamide) and resolved by nonreducing SDS–PAGE or (B) desalting (using gel filtration chromatography with Sephadex G-25), and the remnant peroxidase activity was determined as described under Materials and methods.

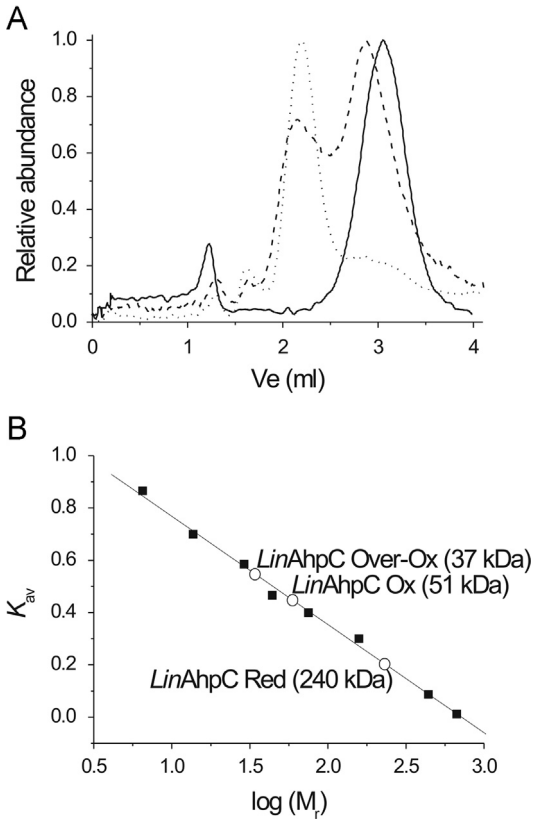

Fig. 7. Redox-dependent oligomeric state of His-tagged *Lin*AhpC. (A) Gel filtration chromatography of redox forms of His-tagged *Lin*AhpC (~40 μM) in a Superdex 200 HP Tricorn column: (dotted line) reduced protein, (dashed line) oxidized protein, and (solid line) overoxidized protein. (B) Plot of K_{av} vs log (M_r) (■) standard proteins and (○) *Lin*AhpC forms. All the standard proteins were from GE Healthcare (filtration calibration kit): thyroglobulin (669 kDa), ferritin (440 kDa), aldolase (158 kDa), conalbumin (75 kDa), ovalbumin (43 kDa), carbonic anhydrase (29 kDa), ribonuclease A (13.7 kDa), and aprotinin (6.5 kDa). (C) Redox-dependent oligomeric state of His-tagged *Lin*AhpC resolved by native PAGE. Protein (10 μM) in standard assay buffer was incubated with various concentrations of H_2O_2 (from 0.02 to 50 mM) in the absence or presence of 100 mM DTT at 25 °C for 15 min.

oligomeric state titration using native PAGE at various H_2O_2 concentrations in the absence or presence of 100 mM DTT. At high concentration of H_2O_2 and DTT, a low-M_r form of *Lin*AhpC was generated (data not shown).

As previously described, the addition of the His-tag affected the sensitivity to inactivation as well as the decamer–dimer equilibrium in other 2-CysPrx proteins from different sources (for example, stabilization of the dodecameric form instead of dimer–decamer equilibrium for human Prx3) [10,30]. Our results suggest that the His-tagged *Lin*AhpC arranges in diverse oligomeric forms depending on its redox state. The reduced protein is decameric and exhibits a tendency to dissociate itself into dimers or monomers upon oxidation or overoxidation, respectively. In addition, a profile similar to the His-tagged *Lin*AhpC was observed

for untagged *Lin*AhpC (using native PAGE) in the absence or presence of DTT and/or H_2O_2 (Supplementary Fig. 4). In the presence of H_2O_2 and DTT, a low-M_r form of untagged *Lin*AhpC was observed, thus further supporting that the addition of an N-terminal His-tag did not affect the redox-dependent oligomeric equilibrium in this protein. This similar profile has been observed for untagged 2-CysPrx from other organisms [31–33].

Redox titration and midpoint reduction potential of His-tagged LinAhpC

Redox titration of His-tagged *Lin*AhpC was performed by incubation of the protein with various molar ratios of reduced and oxidized β-mercaptoethanol (from −318 to −70 mV) (Fig. 8), followed by nonreducing SDS–PAGE and densitometry (Fig. 8A). Using this methodology the midpoint redox potential at pH 7.5 and 30 °C ($E_{m7.5}$) was calculated to be -217 ± 3 mV (see Fig. 8B), which is physiologically coherent compared with that exhibited by the reducing substrate assayed in vitro (*Eco*TRX, $E^{\circ\prime} = -283$ mV [34]). This value is in the range of those reported for other members of the thiol-dependent peroxidases family: −178 mV for AhpC from *Salmonella typhimurium* [25], −192 mV for AhpC from *Treponema pallidum* [35], and −290 mV for human Prx3 [36].

Measurement of the thiol ionization state of His-tagged LinAhpC at 240 nm

Thiolate states of His-tagged *Lin*AhpC were determined by monitoring absorption spectra of reduced and oxidized forms of the protein between 200 and 340 nm in the range of pH 4.5–10 (data not shown). The thiolate anion (but not the thiol form) has a significant absorption at 240 nm [23–25]. Spectra of the reduced and oxidized forms overlapped, except for the region between 240 and 270 nm, in which the absorption of reduced *Lin*AhpC raised up with increasing pH. Changes in ε values reflect ionization of thiol groups (240 nm) and of tyrosine residues (295 nm) as well as protein unfolding (288 nm) [23–25]. Subtraction of values of ε_{240} for oxidized and reduced *Lin*AhpC rendered a titration curve with

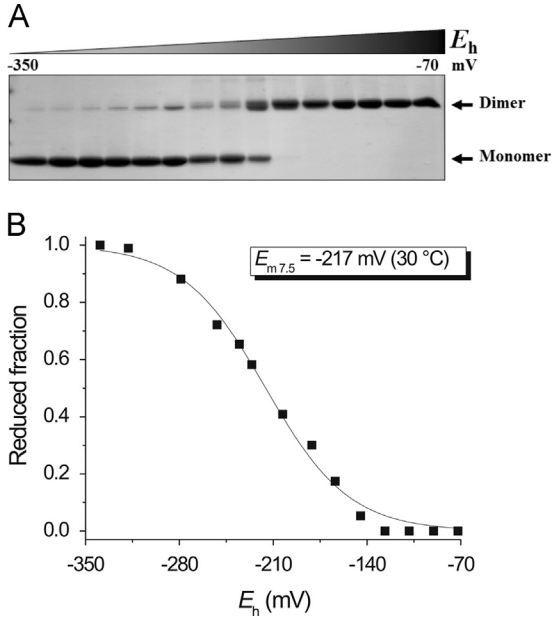

Fig. 8. Redox titration of His-tagged *Lin*AhpC. (A) Nonreducing SDS–PAGE profile of His-tagged *Lin*AhpC (5 μM) incubated at 30 °C and pH 7.5 with various β-mercaptoethanol/HEDS ratios for 4 h. (B) Titration curve was fitted as the reduced fraction versus E_h using a logistic model.

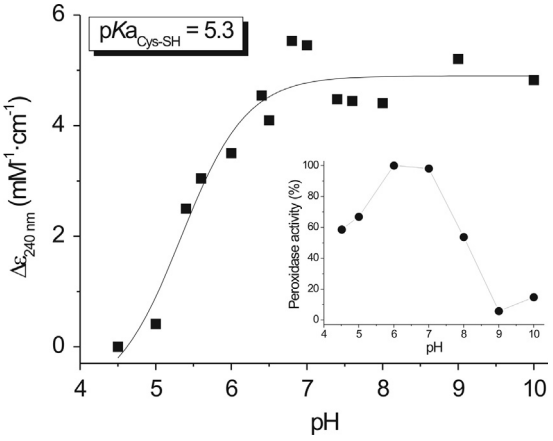

Fig. 9. *Lin*AhpC cysteine thiolate titration by absorption at 240 nm. Thiolate titrations of His-tagged *Lin*AhpC (10 μM) were carried out in 100 mM buffer solution (see Materials and methods) at 25 °C. Inset: pH-dependent profile for thioredoxin peroxidase activity of *Lin*AhpC at 30 °C in 100 mM phosphate buffer.

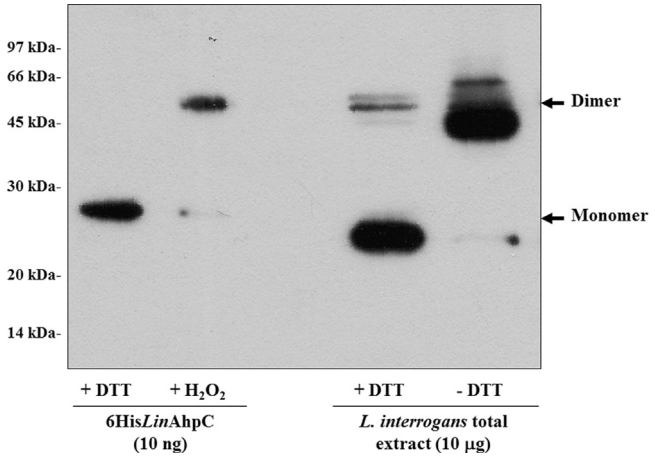

Fig. 10. Immunodetection of *Lin*AhpC in total extract of *L. interrogans*. Approximately 10 μg of protein extract was separated by 15% SDS–PAGE and transferred to a nitrocellulose membrane. The blot was revealed with anti-*Lin*AhpC. As marker control, 10 ng of His-tagged recombinant *Lin*AhpC was used.

one inflection point (Fig. 9), from which was calculated a pK_a value after fitting the data to the Henderson–Hasselbalch equation. Although *Lin*AhpC has two Cys residues the titration curve obtained exhibited a single inflection point, with an average pK_a of 5.3 ± 0.2 (at 25 °C). A possible explanation could be that the two Cys residues have very similar pK_a values and so the inflection points are not separated enough by resolution of the titration curve. [Another explanation could be that C_R may display a high pK_a value, out of the range of the assay employed in this work.]

LinAhpC is a highly expressed protein in L. interrogans and exhibits overoxidation in vivo

Rabbit antisera directed against purified recombinant His-tagged *Lin*AhpC was used to probe and quantitatively evaluate the expression of the protein in Western blots from fresh *L. interrogans* lysates. The detected bands, with apparent M_r of 24 and 45 kDa, were consistent with those predicted for monomeric and covalent dimeric forms of *Lin*AhpC, respectively (Fig. 10). Both bands represent a calculated relative abundance (regarding total proteins) of 0.122 ± 0.006%. Thus, this peroxidase would be a quite abundant protein in the bacterium's cytoplasm

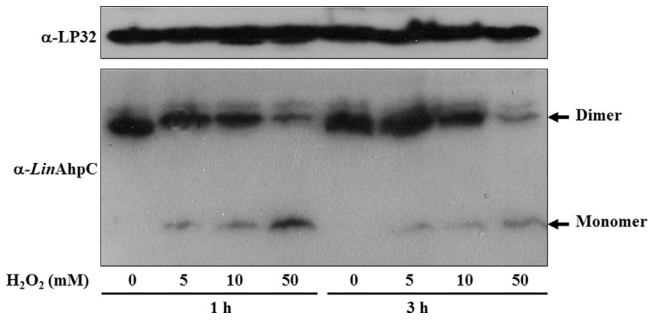

Fig. 11. In vivo *Lin*AhpC redox-state detection. Exponentially growing *L. interrogans* cells were incubated in PBS buffer with various concentrations of H_2O_2 for 1 and 3 h at 28 °C. The cells were lysed with nonreducing SDS–PAGE buffer (in the presence of 10 mM iodoacetamide), and the redox state of *Lin*AhpC was analyzed by Western blot using anti-*Lin*AhpC. LP32 was used as loading control.

and it would constitute a critical molecular tool for the accurate detoxification of H_2O_2 and organic hydroperoxides.

To evaluate overoxidation of *Lin*AhpC in vivo, *L. interrogans* cells (at the exponential phase of growth) were exposed to variable concentrations of H_2O_2 for 1 and 3 h. Fig. 11 shows that in the absence of H_2O_2 *Lin*AhpC was detected in the dimeric (disulfide, active) form. As also shown, the amount of the protein as a dimer decreased after incubation with the peroxide (in a concentration-dependent manner), with a concomitant increase in the monomeric form. This observation is consistent with the results from in vitro experiments (Fig. 5), suggesting that overoxidation of *Lin*AhpC would take place in vivo. On the other hand, the time-dependent accumulation observed for the dimeric form of the protein (Fig. 11) suggests that the expression of the gene encoding *Lin*AhpC would be induced when *L. interrogans* cells are exposed to exogenous H_2O_2. This was supported by quantification of the *Lin*AhpC protein band in reducing SDS–PAGE indicating increases of 1.6 ± 0.1-fold after treatment with the oxidant (data not shown).

Discussion

Although during tissue invasion *L. interrogans* is exposed to soaring concentrations of exogenous reactive oxygen and nitrogen species, which are highly toxic, the pathogen is able to establish a persistent infection in the human host [1,3]. At present, there is a poor understanding about the metabolic pathways related to redox homeostasis in *L. interrogans*. Peroxiredoxins are a family of peroxidases that catalyze the reduction of a variety of hydroperoxides and peroxynitrite using thiols as cosubstrates (for example, glutathione, TRX, tryparedoxin, glutaredoxin, and bacterial AhpF [8,37], among others). The *L. interrogans* genome project gives information on nucleotide sequences encoding peroxiredoxins in this pathogen. We focused on a particular gene that codes for a protein whose deduced amino acid sequence corresponds to a typical 2-CysPrx, having a redox-active site containing the VCP amino acid motif. Thus, as a first approach, we performed the biochemical characterization of this macromolecule (*Lin*AhpC).

Our kinetic data indicated that recombinant *Lin*AhpC possesses peroxidase activity, being able to catalyze the reduction not only of H_2O_2 but also of organic hydroperoxides, such as *t*-bOOH. The leptospiral protein was functional only with TRX (from *E. coli*) as a reducing substrate, being unable to use GSH. The TRX-dependent reduction of the hydroperoxide substrate by *Lin*AhpC exhibited apparent hyperbolic saturation kinetics (for reduced TRX and H_2O_2 or *t*-bOOH). Similarly, the apparent kinetic parameters determined for both substrates are in good agreement with data reported for peroxiredoxin from other organisms [25,35,37–41]. With regard to substrate specificity, the calculated kinetic parameters showed that *Lin*AhpC has a relatively very high affinity for H_2O_2 and *t*-bOOH ($K_{m\ app}$ values of 3–5 μM). In addition, the enzyme exhibited similar $k_{cat}\ K_m^{-1}$ values for hydroperoxide reduction ($3–8 \times 10^5\ M^{-1}\ s^{-1}$). These kinetic properties suggest that the protein would function in vivo to eliminate both H_2O_2 and organic hydroperoxides. This is supported by assays of resistance to oxidative damage performed with transformed *E. coli* cells. By Western blot experiments we determined that functional *Lin*AhpC occurs in vivo as an abundant antioxidant enzyme (~0.12% of the total protein). Our results support that the enzyme would be an important cellular tool for maintaining redox homeostasis in *L. interrogans* living under oxidative conditions.

Considering that *Lin*AhpC is a thiol peroxidase, we evaluated two typical thermodynamic properties. First, we determined a Cys pK_a value of 5.3 (at 25 °C) from measurements of ε_{240}, reflecting the protonation state of a Cys residue in the reduced conformation of the protein. Although *Lin*AhpC has two Cys, only one pK_a value was calculated, which suggests a similar pH dependence for both active residues. This behavior was also reported for *Sal. typhimurium* AhpC [24]. The estimated pK_a value for the thiol moiety of Cys in *Lin*AhpC is characteristic of a typical 2-CysPrx and it suggests that at intracellular pH (about 7.0) ~98% of the thiol Cys is in the thiolate state, which is in parallel with the pK_a values of other C_P [42]. Second, the determined standard redox potential at pH 7.5 for *Lin*AhpC (value of −230 mV) thermodynamically justifies the capacity of this protein to use TRX (average $E^{0\prime}$ of −283 mV [43]) as a reducing substrate. The value of the redox potential determined in this study for *Lin*AhpC is coherent with a flow of reduction equivalents transported through the TRX system, originally from NADPH ($E^{0\prime}$ of −320 mV [34]) to final acceptor substrates, such as hydroperoxides (average $E^{0\prime}$ of 1200 mV).

Inactivation of a typical 2-CysPrx based on overoxidation at the C_P-SH by a peroxide substrate is a consequence of further oxidative events on the C_P-SOH intermediate, producing C_P-SO_2H or C_P-SO_3H [28]. Because the C_P-SO_2H is relatively stable and resistant to reduction by TRX, the protein is no longer able to detoxify peroxides because of the unavailability of the C_P-SH, which plays a primary and central role in attacking the substrate [28,38]. Phylogenetic and biochemical analyses of 2-CysPrx's from diverse species distinguished two types of 2-CysPrx's: robust and sensitive to overoxidation [6]. It has been shown that sensitive Prx's are quickly inactivated by submillimolar concentrations of both hydrogen peroxide and alkyl hydroperoxides. These sensitive 2-CysPrx's present a GG(L/V/I)G and a YF motif, which were found in all eukaryotic organisms analyzed as well as in a few prokaryotes. These structural features accentuate a "kinetic pause" in the disulfide bond formation step, between the C_P-SOH and the C_R-SH. This kinetic pause allows the C_P-SOH group to be exposed longer and can react with a second molecule of peroxide substrate to generate the C_P-SO_2H, facilitating the overoxidation and protein inactivation [6,28,29]. In contrast, the activity of a high number of the typical 2-CysPrx family members from bacteria (such as *Sal. typhimurium* AhpC [25]) is robust, requiring about 100-fold higher hydrogen peroxide concentrations to be inactivated [33]. However, recent studies have shown that peroxiredoxin from cyanobacteria (*Anabaena* sp. and *Synechocystis* sp.) has characteristics of sensitivity to overoxidation, including the presence in its structure of the above-mentioned amino acid consensus sequence [11]. After in silico analysis, we revealed that *Lin*AhpC contained both amino acid motifs GGIG and YF (characteristic of sensitive 2-CysPrx), predicting that the protein would undergo overoxidation. Based on the results of turnover-inactivation assays and nonreducing SDS–PAGE, we verified that the enzyme is inactivated (probably by overoxidation of cysteine residues) by submillimolar concentrations of H_2O_2 with a significant reduction in peroxidase activity ($C_{hyp\ 1\%} = \sim 30$ μM). Some typical 2-CysPrx's from bacteria and

eukaryotes undergo redox-sensitive oligomerization [10,31,35]. Reduced or overoxidized forms of the enzyme arrange in a decameric state, whereas the disulfide-bond form mainly produces a dimer [33]. Although *Lin*AhpC presented sensitivity to redox oligomerization, it exhibited a structural transition from pentadimer to dimer with changes going from a reduced (thiol) to an oxidized (disulfide) state. The overoxidized enzyme (inactive) was arranged in an apparent dimer/monomer mixture, which was stimulated by a high concentration of peroxide and reducing substrates. These results suggest that *Lin*AhpC could lack chaperone activity in vivo under conditions of oxidative stress, because of its inability to form high-M_r oligomeric states.

According to the floodgate model [7], the peroxidase activity of 2-CysPrx constitutes a "wall" preventing the effects of H_2O_2 (and related oxidants) on peroxide-sensitive targets. Overoxidation of 2-CysPrx (by elevated levels of peroxide) allows peroxide to "break the wall," enabling the activation or inactivation of biological targets. This model is based (in part) on the notion that eukaryotic 2-CysPrx's have evolved to become more sensitive to inactivation by overoxidation. However, there are several recent data in the literature (and results herein) supporting that sensitive 2-CysPrx's are not exclusive to eukaryotic organisms. The GG(L/V/I)G and/or YF motif characteristic of sensitive 2-CysPrx's are not exclusive to eukaryotic organisms. The wide distribution of 2-CysPrx's predicted to be sensitive among prokaryotes suggests that this structural feature appeared early during evolution. Several sensitive 2-CysPrx's from other pathogenic bacteria such as *H. pylori* exhibit chaperone activity in the overoxidized state, thus contributing to stabilization of proteins under oxidative stress [10,12,44]. Therefore, more studies are required to establish the relationships between 2-CysPrx overoxidation (redox sensitivity) and redox-dependent signaling in prokaryote organisms.

In view of the results we have obtained (plus data in the literature), many questions arise: why does *L. interrogans* (as a pathogenic bacterium) have a sensitive 2-CysPrx? Are there H_2O_2-dependent signaling mechanisms in this bacterium? Is this protein involved in some of them? Are there overoxidized 2-CysPrx rescue mechanisms in this prokaryote? In this scenario, we can hypothesize that the *Lin*AhpC could operate as a wall containing H_2O_2 according to the floodgate model in *L. interrogans*. Moreover, the formation of overoxidized *Lin*AhpC (peroxidase-inactive monomer/compact dimer) could be itself an oxidative stress signal that acts as a second messenger regulating various signaling pathways. This type of mechanism has been observed for different enzymes (for example, glyceraldehyde-3-P dehydrogenase), which after being chemically modified (e.g., by overoxidation) acquire cell signaling functions [45–47]. We are focusing our studies with the aim of providing in-depth answers to the above-stated questions.

Acknowledgments

This work was supported by grants from the Universidad Nacional del Litoral (CAI+D Orientados & Redes), CONICET (PIP112-2011-0100439, PIP114-2011-0100168), and ANPCyT (PICT2012-2439). A.R. is an undergraduate student from the UNL. N.S. and M.D.H. are fellows from CONICET. D.G.A., A.A.I., and S.A.G. are investigator career members from CONICET.

Appendix A. Supplementary material

Supplementary data associated with this article can be found in the online version at http://dx.doi.org/10.1016/j.freeradbiomed.2014.08.014.

References

[1] Feigin, R. D.; Anderson, D. C. Human leptospirosis. *CRC Crit. Rev. Clin. Lab. Sci.* **5:**413–467; 1975.
[2] Ren, S. X.; Fu, G.; Jiang, X. G.; Zeng, R.; Miao, Y. G.; Xu, H.; Zhang, Y. X.; Xiong, H.; Lu, G.; Lu, L. F.; Jiang, H. Q.; Jia, J.; Tu, Y. F.; Jiang, J. X.; Gu, W. Y.; Zhang, Y. Q.; Cai, Z.; Sheng, H. H.; Yin, H. F.; Zhang, Y.; Zhu, G. F.; Wan, M.; Huang, H. L.; Qian, Z.; Wang, S. Y.; Ma, W.; Yao, Z. J.; Shen, Y.; Qiang, B. Q.; Xia, Q. C.; Guo, X. K.; Danchin, A.; Saint Girons, I.; Somerville, R. L.; Wen, Y. M.; Shi, M. H.; Chen, Z.; Xu, J. G.; Zhao, G. P. Unique physiological and pathogenic features of *Leptospira interrogans* revealed by whole-genome sequencing. *Nature* **422:**888–893; 2003.
[3] Eshghi, A.; Lourdault, K.; Murray, G. L.; Bartpho, T.; Sermswan, R. W.; Picardeau, M.; Adler, B.; Snarr, B.; Zuerner, R. L.; Cameron, C. E. *Leptospira interrogans* catalase is required for resistance to H_2O_2 and for virulence. *Infect. Immun.* **80:**3892–3899; 2012.
[4] Faine, S. Catalase activity in pathogenic Leptospira. *J. Gen. Microbiol.* **22:**1–9; 1960.
[5] Rao, P. J.; Larson, A. D.; Cox, C. D. Catalase activity in Leptospira. *J. Bacteriol.* **88:**1045–1048; 1964.
[6] Wood, Z. A.; Schroder, E.; Robin Harris, J.; Poole, L. B. Structure, mechanism and regulation of peroxiredoxins. *Trends Biochem. Sci.* **28:**32–40; 2003.
[7] Hall, A.; Karplus, P. A.; Poole, L. B. Typical 2-Cys peroxiredoxins—structures, mechanisms and functions. *FEBS J.* **276:**2469–2477; 2009.
[8] Aran, M.; Ferrero, D. S.; Pagano, E.; Wolosiuk, R. A. Typical 2-Cys peroxiredoxins—modulation by covalent transformations and noncovalent interactions. *FEBS J.* **276:**2478–2493; 2009.
[9] Nelson, K.J.; Knutson, S.T.; Soito, L.; Klomsiri, C.; Poole, L.B.; Fetrow, J.S. Analysis of the peroxiredoxin family: using active-site structure and sequence information for global classification and residue analysis. Proteins **79:**947-964.
[10] Barranco-Medina, S.; Lazaro, J. J.; Dietz, K. J. The oligomeric conformation of peroxiredoxins links redox state to function. *FEBS Lett.* **583:**1809–1816; 2009.
[11] Pascual, M. B.; Mata-Cabana, A.; Florencio, F. J.; Lindahl, M.; Cejudo, F. J. Overoxidation of 2-Cys peroxiredoxin in prokaryotes: cyanobacterial 2-Cys peroxiredoxins sensitive to oxidative stress. *J. Biol. Chem.* **285:**34485–34492; 2010.
[12] Chuang, M. H.; Wu, M. S.; Lo, W. L.; Lin, J. T.; Wong, C. H.; Chiou, S. H. The antioxidant protein alkylhydroperoxide reductase of *Helicobacter pylori* switches from a peroxide reductase to a molecular chaperone function. *Proc. Natl. Acad. Sci. USA* **103:**2552–2557; 2006.
[13] Ellinghausen Jr H. C.; McCullough, W. G. Nutrition of Leptospira pomona and growth of 13 other serotypes: fractionation of oleic albumin complex and a medium of bovine albumin and polysorbate 80. *Am. J. Vet. Res.* **26:**45–51; 1965.
[14] Johnson, R.; Harris, V. Differentiation of pathogenic and saprophytic leptospires. I. Growth at low temperatures. *J. Bacteriol.* **94:**27–31; 1967.
[15] Louvel, H.; Picardeau, M. Genetic manipulation of *Leptospira biflexa*. (Unit 12E). *Curr. Protoc. Microbiol.* **Chapter 12:**14; 2007.
[16] Holmgren, A.; Bjornstedt, M. Thioredoxin and thioredoxin reductase. *Methods Enzymol.* **252:**199–208; 1995.
[17] Laemmli, U. K. Cleavage of structural proteins during the assembly of the head of bacteriophage T4. *Nature* **227:**680–685; 1970.
[18] Arndt, C.; Koristka, S.; Bartsch, H.; Bachmann, M. Native polyacrylamide gels. *Methods Mol. Biol.* **869:**49–53; 2012.
[19] Bradford, M. M. A rapid and sensitive method for the quantitation of microgram quantities of protein utilizing the principle of protein–dye binding. *Anal. Biochem.* **72:**248–254; 1976.
[20] Eyer, P.; Worek, F.; Kiderlen, D.; Sinko, G.; Stuglin, A.; Simeon-Rudolf, V.; Reiner, E. Molar absorption coefficients for the reduced Ellman reagent: reassessment. *Anal. Biochem.* **312:**224–227; 2003.
[21] Vaitukaitis, J.; Robbins, J. B.; Nieschlag, E.; Ross, G. T. A method for producing specific antisera with small doses of immunogen. *J. Clin. Endocrinol. Metab.* **33:**988–991; 1971.
[22] Arias, D. G.; Cabeza, M. S.; Erben, E. D.; Carranza, P. G.; Lujan, H. D.; Tellez Inon, M. T.; Iglesias, A. A.; Guerrero, S. A. Functional characterization of methionine sulfoxide reductase A from *Trypanosoma* spp. *Free Radic. Biol. Med.* **50:**37–46; 2011.
[23] Arias, D. G.; Marquez, V. E.; Chiribao, M. L.; Gadelha, F. R.; Robello, C.; Iglesias, A. A.; Guerrero, S. A. Redox metabolism in *Trypanosoma cruzi:* functional characterization of tryparedoxins revisited. *Free Radic. Biol. Med.* **63C:**65–77; 2013.
[24] Nelson, K. J.; Parsonage, D.; Hall, A.; Karplus, P. A.; Poole, L. B. Cysteine pK (a) values for the bacterial peroxiredoxin AhpC. *Biochemistry* **47:**12860–12868; 2008.
[25] Parsonage, D.; Karplus, P. A.; Poole, L. B. Substrate specificity and redox potential of AhpC, a bacterial peroxiredoxin. *Proc. Natl. Acad. Sci. USA* **105:**8209–8214; 2008.
[26] Arias, D. G.; Regner, E. L.; Iglesias, A. A.; Guerrero, S. A. *Entamoeba histolytica* thioredoxin reductase: molecular and functional characterization of its atypical properties. *Biochim. Biophys. Acta* **1820:**1859–1866; 2012.
[27] Gouy, M.; Guindon, S.; Gascuel, O. SeaView version 4: a multiplatform graphical user interface for sequence alignment and phylogenetic tree building. *Mol. Biol. Evol.* **27:**221–224; 2010.
[28] Nelson, K. J.; Parsonage, D.; Karplus, P. A.; Poole, L. B. Evaluating peroxiredoxin sensitivity toward inactivation by peroxide substrates. *Methods Enzymol.* **527:**21–40; 2013.

[29] Peskin, A. V.; Dickerhof, N.; Poynton, R. A.; Paton, L. N.; Pace, P. E.; Hampton, M. B.; Winterbourn, C. C. Hyperoxidation of peroxiredoxins 2 and 3: rate constants for the reactions of the sulfenic acid of the peroxidatic cysteine. *J. Biol. Chem.* **288:**14170–14177; 2013.
[30] Konig, J.; Galliardt, H.; Jutte, P.; Schaper, S.; Dittmann, L.; Dietz, K. J. The conformational bases for the two functionalities of 2-cysteine peroxiredoxins as peroxidase and chaperone. *J. Exp. Bot.* **64:**3483–3497; 2013.
[31] Wood, Z. A.; Poole, L. B.; Hantgan, R. R.; Karplus, P. A. Dimers to doughnuts: redox-sensitive oligomerization of 2-cysteine peroxiredoxins. *Biochemistry* **41:**5493–5504; 2002.
[32] Parsonage, D.; Youngblood, D. S.; Sarma, G. N.; Wood, Z. A.; Karplus, P. A.; Poole, L. B. Analysis of the link between enzymatic activity and oligomeric state in AhpC, a bacterial peroxiredoxin. *Biochemistry* **44:**10583–10592; 2005.
[33] Hall, A.; Nelson, K.; Poole, L. B.; Karplus, P. A. Structure-based insights into the catalytic power and conformational dexterity of peroxiredoxins. *Antioxid. Redox Signaling* **15:**795–815; 2011.
[34] Cheng, Z.; Arscott, L. D.; Ballou, D. P.; Williams Jr. C. H. The relationship of the redox potentials of thioredoxin and thioredoxin reductase from *Drosophila melanogaster* to the enzymatic mechanism: reduced thioredoxin is the reductant of glutathione in Drosophila. *Biochemistry* **46:**7875–7885; 2007.
[35] Parsonage, D.; Desrosiers, D. C.; Hazlett, K. R.; Sun, Y.; Nelson, K. J.; Cox, D. L.; Radolf, J. D.; Poole, L. B. Broad specificity AhpC-like peroxiredoxin and its thioredoxin reductant in the sparse antioxidant defense system of *Treponema pallidum*. *Proc. Natl. Acad. Sci. USA* **107:**6240–6245; 2010.
[36] Cox, A. G.; Peskin, A. V.; Paton, L. N.; Winterbourn, C. C.; Hampton, M. B. Redox potential and peroxide reactivity of human peroxiredoxin 3. *Biochemistry* **48:**6495–6501; 2009.
[37] Hofmann, B.; Hecht, H. J.; Flohe, L. Peroxiredoxins. *Biol. Chem.* **383:**347–364; 2002.
[38] Manta, B.; Hugo, M.; Ortiz, C.; Ferrer-Sueta, G.; Trujillo, M.; Denicola, A. The peroxidase and peroxynitrite reductase activity of human erythrocyte peroxiredoxin 2. *Arch. Biochem. Biophys.* **484:**146–154; 2009.
[39] Arias, D. G.; Carranza, P. G.; Lujan, H. D.; Iglesias, A. A.; Guerrero, S. A. Immunolocalization and enzymatic functional characterization of the thioredoxin system in *Entamoeba histolytica*. *Free Radic. Biol. Med.* **45:**32–39; 2008.
[40] Pineyro, M. D.; Arcari, T.; Robello, C.; Radi, R.; Trujillo, M. Tryparedoxin peroxidases from *Trypanosoma cruzi:* high efficiency in the catalytic elimination of hydrogen peroxide and peroxynitrite. *Arch. Biochem. Biophys.* **507:**287–295; 2011.
[41] Baker, L. M.; Raudonikiene, A.; Hoffman, P. S.; Poole, L. B. Essential thioredoxin-dependent peroxiredoxin system from *Helicobacter pylori:* genetic and kinetic characterization. *J. Bacteriol.* **183:**1961–1973; 2001.
[42] Ferrer-Sueta, G.; Manta, B.; Botti, H.; Radi, R.; Trujillo, M.; Denicola, A. Factors affecting protein thiol reactivity and specificity in peroxide reduction. *Chem. Res. Toxicol.* **24:**434–450; 2011.
[43] Cheng, Z.; Zhang, J.; Ballou, D. P.; Williams Jr. C. H. Reactivity of thioredoxin as a protein thiol–disulfide oxidoreductase. *Chem. Rev.* **111:**5768–5783; 2011.
[44] Rhee, S. G.; Woo, H. A. Multiple functions of peroxiredoxins: peroxidases, sensors and regulators of the intracellular messenger H_2O_2, and protein chaperones. *Antioxid. Redox Signaling* **15:**781–794; 2011.
[45] Holtgrefe, S.; Gohlke, J.; Starmann, J.; Druce, S.; Klocke, S.; Altmann, B.; Wojtera, J.; Lindermayr, C.; Scheibe, R. Regulation of plant cytosolic glyceraldehyde 3-phosphate dehydrogenase isoforms by thiol modifications. *Physiol. Plant* **133:**211–228; 2008.
[46] Sirover, M. A. On the functional diversity of glyceraldehyde-3-phosphate dehydrogenase: biochemical mechanisms and regulatory control. *Biochim. Biophys. Acta* **1810:**741–751; 2011.
[47] Sirover, M. A. New insights into an old protein: the functional diversity of mammalian glyceraldehyde-3-phosphate dehydrogenase. *Biochim. Biophys. Acta* **1432:**159–184; 1999.